

# Molecular Conformation in Oligo(ethylene glycol)-Terminated Self-Assembled Monolayers on Gold and Silver Surfaces Determines Their Ability To Resist Protein Adsorption

P. Harder, M. Grunze,\* and R. Dahint

Angewandte Physikalische Chemie, Universität Heidelberg, INF 253, D 69120 Heidelberg, Germany

G. M. Whitesides

Department of Chemistry, Harvard University, Cambridge, Massachusetts 02138

P. E. Laibinis

Department of Chemical Engineering, Massachusetts Institute of Technology, Cambridge, Massachusetts 02139

Received: August 12, 1997<sup>⊗</sup>

We report data from infrared absorption (FTIR) and X-ray photoelectron spectroscopies that correlate the molecular conformation of oligo(ethylene glycol) (OEG)-terminated self-assembled alkanethiolate monolayers (SAMs) with the ability of these films to resist protein adsorption. We studied three different SAMs of alkanethiolates on both evaporated Au and Ag surfaces. The SAMs were formed from substituted 1-undecanethiols with either a hydroxyl-terminated hexa(ethylene glycol) (EG6-OH) or a methoxy-terminated tri(ethylene glycol) (EG3-OMe) end group, or a substituted 1-tridecanethiol chain with a methoxy-terminated tri(ethylene glycol) end group and a  $-\text{CH}_2\text{OCH}_3$  side chain at the C-12 atom (EG[3,1]-OMe). The infrared data of EG6-OH-terminated SAMs on both Au and Ag surfaces reveal the presence of a crystalline helical OEG phase, coexisting with amorphous OEG moieties; the EG[3,1]-OMe-terminated alkanethiolates on Au and Ag show a lower absolute coverage and greater disorder than the two other compounds. The molecular conformation of the methoxy-terminated tri(ethylene glycol) (EG3-OMe) is different on Au and Ag surfaces due to the different lateral densities of SAMs on these substrates: on Au we find a conformation similar to that of EG6-OH alkanethiolates, whereas on Ag the infrared spectra indicate a densely packed film with trans conformation around the C–C bonds of the glycol units. The resistance of these OEG-functionalized alkanethiolate SAMs to adsorption of fibrinogen from a buffered solution correlates with the molecular conformation of the OEG moieties. The predominantly crystalline helical and the amorphous forms of OEG on gold substrates are resistant to adsorption of proteins, while a densely packed “all-trans” form of EG3-OMe present on silver surfaces adsorbs protein. The experimental observations are compatible with the hypothesis that binding of interfacial water by the OEG moieties is important in their ability to resist protein adsorption.

## 1. Introduction

A well-known strategy for rendering surfaces protein resistant involves incorporation of poly(ethylene glycol),<sup>1–3</sup> (PEG) both into polymers and as surface-grafted chains.<sup>4</sup> The resistance of PEG to the adsorption of proteins is generally considered a steric repulsion effect, where the polymer prevents the protein from reaching the substrate surface to adsorb.<sup>5–7</sup> Jeon et al. considered the balance between steric repulsion, van der Waals attraction, and hydrophobic interaction between protein in solution and the PEG surface. They found that the net force determining the adsorption of the PEG-presenting surface depends on the thickness of the grafted layers and their surface coverage. The steric repulsion has an osmotic (due to the solvation of the PEG chains) and an elastic (due to the conformational entropy of the PEG chains) component; these components become effective when the protein reaches the interphase by diffusion and compresses the PEG layer. The van der Waals contribution to the attractive force was found to

be smaller than the hydrophobic interaction between the protein and the hydrophobic surface, so only the latter was considered to compete with the steric repulsion effect. Protein resistance was only observed for the room-temperature stable hydrated phase of PEG in its helical (gauche–trans–gauche) conformation, and not for the high-temperature dehydrated amorphous phase.<sup>8</sup>

Luesse and Arnold<sup>9</sup> applied proton and deuterium NMR relaxation time measurements to determine the number of water molecules per ethylene glycol repeat unit ( $-\text{CH}_2\text{CH}_2-\text{O}-$ ) in PEG. The maximum water content was one molecule per ethylene glycol unit. Water bridges neighboring PEG strands via two hydrogen bonds to the oxygen atoms of two neighboring PEG chains at lower water content. The activation barrier between the energy of one and two hydrogen bonds was found in these NMR studies to be 34 kJ/mol. The bridge-bonded water molecules are stable to a temperature of 330 K; above this temperature their signature in the NMR experiments vanishes.

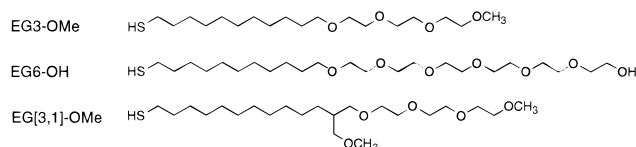
The “steric repulsion” effect that prevents protein adsorption onto PEG chains attached to a surface is related to the positive

<sup>⊗</sup> Abstract published in *Advance ACS Abstracts*, December 15, 1997.

free energy associated with compression (and therefore restriction of configurational freedom) and concomitant desolvation when the protein tries to attach to the surface. In a laterally densely packed film with only a few ethylene glycol units per chain attached to the surface, the steric repulsion will be (in absolute terms) smaller because of conformational constraints and the reduced hydration energy per chain and unit surface. It is therefore of interest to test experimentally if complete conformational freedom of the grafted polymer chains is necessary for the ability of an ethylene glycol coated surface to resist protein adsorption or if protein resistance of PEG is inherent in its composition and molecular conformation.

That the latter might be the case was suggested by the protein resistance of oligo(ethylene glycol)-terminated self-assembled monolayers (SAMs) as first described by Prime and Whitesides.<sup>10</sup> Prime and Whitesides compared and correlated the surface composition of different functionalized alkanethiolate SAMs with the amount of protein adsorbed from a single-component protein solution and found that both the hydroxyl- and the methoxy-terminated oligo(ethylene glycol) (OEG) SAMs showed protein resistance, even when the surface layer was diluted with *n*-alkanethiol molecules up to a surface coverage of 35%. These results demonstrate that resistance to protein adsorption is insensitive to the surface density of OEG groups over a substantial range of surface compositions. A detailed model to account for the protein resistance of the OEG SAMs was not derived from these measurements.

In this paper, we discuss evidence correlating the molecular conformation of oligo(ethylene glycol)-terminated self-assembled alkanethiolate monolayers with the ability of these films to resist protein adsorption. We made SAMs on both evaporated Au and Ag surfaces from three different thiols and measured their wetting properties and the tendency of fibrinogen to adsorb on them.



Two of them were substituted 1-undecanethiols with either a hydroxyl-terminated hexa(ethylene glycol) (EG6-OH) or a methoxy-terminated tri(ethylene glycol) (EG3-OMe) end group. The third thiol had a 1-tridecanethiol chain with a methoxy-terminated tri(ethylene glycol) end group and a  $-\text{CH}_2\text{OCH}_3$  side chain at the C-12 atom (EG[3,1]-OMe). A racemic mixture of the two possible enantiomers around the C-12 atom was used in our study.

Our measurements show that the protein resistance of OEG-functionalized alkanethiolate SAMs is related to the molecular conformation of the OEG moieties. The films consisting of predominantly crystalline helical and amorphous OEG on gold substrates are protein resistant, whereas a densely packed and preferentially "all-trans" form present on silver surfaces adsorbs protein. The experimental observations suggest that interfacial water adsorption on the OEG moieties in the alkanethiolate SAMs is important for their ability to resist adsorption.<sup>11</sup>

## 2. Experimental Section

**2.1. Sample Preparation.** Polycrystalline Au and Ag (200 nm) films were prepared by evaporation of the metals onto test grade, 100 mm, single polished silicon wafers (Silicon Sense) coated with an adhesion layer of titanium (20 nm). The

evaporations were performed at a pressure of  $2 \times 10^{-7}$  mbar and a rate of 0.5 nm/s for both metals.

1-Hexanethiol (Merck, >97%), 1-decanethiol (Fluka, >95%), 1-dodecanethiol (Sigma, 98%), 1-hexadecanethiol (Fluka, 90–95%), and 1-octadecanethiol (Aldrich, 98%) were used as received. The syntheses of 1-docosanethiol,  $\text{HS}(\text{CH}_2)_{11}(\text{OCH}_2\text{CH}_2)_6\text{OH}$  (EG6-OH),  $\text{HS}(\text{CH}_2)_{11}(\text{OCH}_2\text{CH}_2)_3\text{OCH}_3$  (EG3-OMe), and  $\text{HS}(\text{CH}_2)_{11}\text{CH}(\text{CH}_2\text{OCH}_3)\text{CH}_2(\text{OCH}_2\text{CH}_2)_3\text{OCH}_3$  (EG[3,1]-OMe) have been described elsewhere.<sup>12–14</sup> Perdeuterated hexadecanethiol-*d*<sub>33</sub>, prepared from the corresponding perdeuterated bromide, was available from previous studies.<sup>15</sup> Poly(ethylene glycol) 8000 was supplied from Serva.

The gold and silver substrates were cut into pieces ( $\approx 2$  cm  $\times$  2 cm) with a diamond-tipped stylus, dusted free of debris with N<sub>2</sub>, rinsed with analytical grade ethanol, and immersed in 10 mL of a 2 mmol solution of the thiol in 50 mL screw-top vials. The oligo(ethylene glycol)-terminated SAMs were prepared from an ethanolic solution; unfunctionalized alkanethiolates for the XPS reference curve were prepared from hexane solution.<sup>16</sup> The vials with the thiol solutions were stored in the dark at ambient temperature.<sup>17</sup> The volume above the thiol solution was filled with air. After removal from the thiol solution, the SAMs were rinsed with the pure solvent and blown dry with N<sub>2</sub>.

**2.2. Characterization of the SAMs.** Water contact angles were measured 30 min after removal from the thiol solution with a Kruss Model G1 goniometer-microscope at room temperature in a water vapor saturated atmosphere. Droplets were dispensed from a microburet, and the reported values are the average of three advancing contact angle measurements taken at different locations on the SAM with the tip in contact with the drop.

Fourier transform infrared reflection absorption spectroscopy (FTIRAS) has been widely used to examine the orientation and average conformation of thin adsorbed films on metal surfaces<sup>18</sup> and is well suited to study the relationship between molecular orientation, conformation, and protein adsorption. Only the component of the vibrational transition dipole moments perpendicular to the surface plane contributes to the absorption spectra; that is, the intensity of an absorption band is proportional to the squared cosine of the angle between the transition dipole moment and the surface normal.<sup>19</sup> The internal molecular conformation affects the position of the absorption maxima, so that the absorption bands can be correlated with a specific molecular conformation by comparison with reference data. In the present study, we investigate the molecular conformation and orientation (with respect to the surface plane) of the oligo(ethylene glycol) moiety of the molecules. As reference, we use the vibrational data reported for poly(ethylene glycol). The low-temperature hydrated crystalline phase of poly(ethylene glycol) has a preferential helical conformation as a result of glycol moieties with a trans conformation around the C–O bonds and a gauche conformation around the C–C bond (TGT).<sup>20</sup> Above  $\sim 60$  °C, the crystalline/amorphous phase transition temperature, the predominant conformation around the C–C bond is still gauche, but the C–O bond can be trans or gauche (TGT, TGG, GGT) and the sign of the C–C gauche rotational angle is not uniform (gauche(+), gauche(–)).<sup>21</sup> Both phases have a characteristic signature in the vibrational frequencies and intensities of the ethylene glycol units.

Infrared spectra were taken with two dry air purged Bio-Rad spectrometers, Model FTS 175c. Both instruments were equipped with a liquid nitrogen cooled MCT detector, a polarizer constructed of an aluminum wire grid on a KRS-5 substrate,

and an accessory for grazing angle reflectance spectroscopy (Bio-Rad Universal Reflectance Accessory and Pike grazing angle accessory AGA). Spectra were taken by coadding 1024 scans at a resolution of  $2\text{ cm}^{-1}$  and ratioed against the spectra of a  $n\text{-C}_{16}\text{D}_{35}\text{S}$ -SAM. Negative absorption bands in the spectra at  $2050\text{--}2200\text{ cm}^{-1}$  are due to the C–D absorptions for the perdeuterated reference sample. The perdeuterated hexadecanethiolate- $d_{33}$  film removes airborne contaminations on the reference sample and does not absorb in the spectral regions of interest.

X-ray photoelectron spectra were obtained with an Leybold-Heraeus LHS-11 system using a Mg  $K\alpha$  source and a multi-channel detector at a takeoff angle of  $90^\circ$  relative to the surface. The base pressure in the analysis chamber during the measurements was below  $6 \times 10^{-9}$  mbar. C 1s and O 1s detail spectra were averaged over 10 scans. Two scans were accumulated for the Ag 3d and Au 4d spectra. The step width and pass energy were set at 0.1 and 23 eV, respectively, giving an experimental resolution of  $\sim 1$  eV. The duration of X-ray exposure for a series of C 1s, O 1s, and substrate (Au 4d, Ag 3d) detailed spectra was 15 min.

The relative ratio of alkyl C 1s signal at 284.9 eV and ether C 1s signal at 286.8 eV was determined by a numerical least-squares fitting routine using normalized reference spectra of a poly(ethylene glycol) 8000 bulk sample for the ether C 1s peak and a dodecanethiolate SAM for the alkyl C 1s peak shape.

**2.3. Protein Adsorption Experiments.** After the initial IR measurement to characterize the films, the samples were cut into two pieces. One piece was placed on the bottom of a 15 mL glass vial and covered with 2 mL of distilled water. The vial was subsequently filled with a solution of fibrinogen in PBS buffer (1 mg/mL). After 15 min of immersion, a water hose was inserted and the vial volume exchanged several times to avoid a Langmuir–Blodgett-like transfer of protein at the air–water interface when the sample was removed. After drying in a stream of  $\text{N}_2$ , the sample was again investigated by IR to quantify the amount of adsorbed fibrinogen by the height of the amide I and amide II bands<sup>22</sup> at  $1660$  and  $1540\text{ cm}^{-1}$  in the difference spectra, respectively. The coverages reported in this work were normalized to the maximum adsorption coverage of fibrinogen on dodecanethiolate SAMs. Surface plasmon resonance (SPR) measurements gave an average signal of 3500 resonance units for the nonspecific adsorption of fibrinogen on alkanethiolates. According to the manufacturer (Pharmacia), this signal corresponds to a coverage of ca.  $3.5\text{ ng protein/mm}^2$ .<sup>23</sup>

### 3. Results

**3.1. Contact Angle Measurements.** The values for the advancing contact angle of water ( $\theta_a(\text{H}_2\text{O})$ ) 30 min after removal of the samples from the ethanolic thiol solutions were  $30\text{--}35^\circ$  for EG6-OH,  $63^\circ \pm 2^\circ$  for EG3-OMe, and  $57^\circ \pm 2^\circ$  for EG-[3,1]-OMe, respectively. The substrate (Au or Ag) had no influence on the water contact angle. The contact angles for EG6-OH and EG3-OMe reflect the different hydrophilicities of the terminal groups (OH or  $\text{OCH}_3$ ) on the ethylene glycol moieties. The EG6-OH surface is less hydrophilic than OH-terminated alkanethiolate SAMs ( $\theta_a(\text{H}_2\text{O}) < 15^\circ$ )<sup>24</sup> and the EG3-OMe surface is less hydrophobic than  $\omega$ -methoxyalkanethiolate SAMs ( $\theta_a(\text{H}_2\text{O}) = 83^\circ$  on Au and  $85^\circ$  on Ag).<sup>25</sup> The differences in contact angle between the –OH- and – $\text{OCH}_3$ -terminated alkanethiolates and the oligo(ethylene glycol)-terminated alkanethiolates with the same functional group can be rationalized by the exposure of the methylene groups and oxygen atom of the terminal ethylene glycol units at the outer surface, respec-

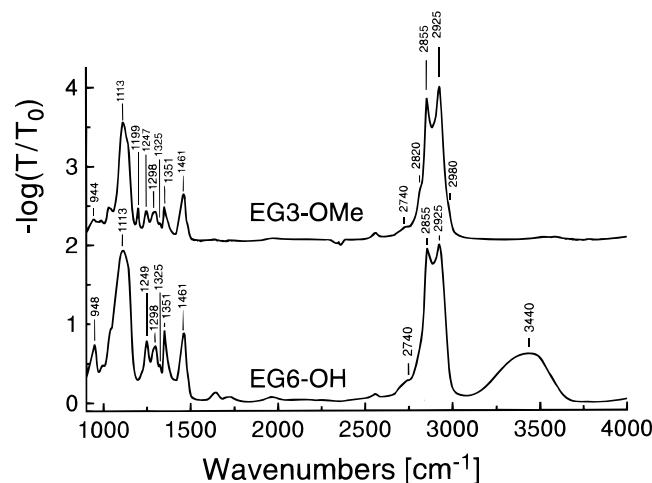


**Figure 1.** IR spectra of neat liquid EG3-OMe (upper curve) and EG6-OH (lower curve).

tively. The lower contact angle of EG[3,1]-OMe as compared to EG3-OMe indicates a disordered layer with more ether oxygen atoms accessible to the liquid. A disordered ether phase is also indicated by FTIR spectra discussed below.

**3.2. Infrared Spectroscopy.** For the discussion of the vibrational spectra of the EG-terminated SAMs, we will refer to the band assignments of unfunctionalized alkanethiols<sup>26</sup> and poly(ethylene glycol).<sup>2</sup> As a reference for the SAM spectra, we show transmission spectra of neat liquid EG6-OH and EG3-OMe in Figure 1. The bands at  $2855$  and  $2925\text{ cm}^{-1}$  are ascribed to the symmetric and asymmetric  $\text{CH}_2$ -stretching bands of the  $\text{C}_{11}$ -methylene units, respectively. The methylene stretching frequencies are representative for a liquid with gauche and trans conformations<sup>27</sup> in the alkyl chain. Crystalline alkane chains with an all-trans conformation, such as in well-ordered alkanethiolate films, absorb at  $2850$  and  $2917\text{ cm}^{-1}$ .<sup>15</sup> The  $\text{CH}_2$ -stretching vibrations of the OEG molecular entities are expected to give a broad band at ca.  $2865\text{ cm}^{-1}$  with a shoulder at  $2930\text{ cm}^{-1}$ ,<sup>28</sup> but these features are masked by the sharper alkane  $\text{CH}_2$ -stretching bands.

The C–O–C stretching vibration gives a very strong absorption band at  $1113\text{ cm}^{-1}$ . The band at  $1461\text{ cm}^{-1}$  is dominated by the  $\text{CH}_2$ -scissoring modes of the ether methylene units. The shoulder at the high-frequency side is attributed to the corresponding vibration of the alkyl methylene units at  $1467\text{ cm}^{-1}$ . Bands at  $1351$  and  $948\text{ cm}^{-1}$  (EG6-OH)/ $944\text{ cm}^{-1}$  (EG3-OMe) are associated with the ether  $\text{CH}_2$ -wagging and rocking modes. The ether  $\text{CH}_2$ -twisting modes occur at  $1298$  and  $1247\text{--}1249\text{ cm}^{-1}$ . All the OEG-derived  $\text{CH}_2$ -bending mode positions are within  $\pm 2\text{ cm}^{-1}$  of the corresponding band positions for molten or amorphous<sup>29</sup> poly(ethylene glycol). Specific for the – $\text{OCH}_3$ -terminated EG3-OMe is the methyl-rocking mode at  $1199\text{ cm}^{-1}$ .<sup>30</sup> The EG6-OH spectrum shows a broad OH-stretching band<sup>31</sup> at  $\sim 3440\text{ cm}^{-1}$ .

**3.2.1. EG6-OH SAMs on Gold and Silver Surfaces.** The films prepared from the EG6-OH oligo(ethylene glycol) alkanethiols on gold surfaces show a high degree of variation in their molecular conformation. Figures 2 and 3 show the range of differences in the FTIR data of ca. 100 samples of EG6-OH prepared from ethanol solutions with various immersion times and concentrations. The spectra displayed in Figures 2 and 3 are representative for different degrees of crystallinity and molecular orientations in the EG6-OH films. Spectra 2a and b were taken on samples adsorbed from a 2 mmol ethanolic solution after 1 min and 2 days immersion time, respectively.<sup>32</sup>

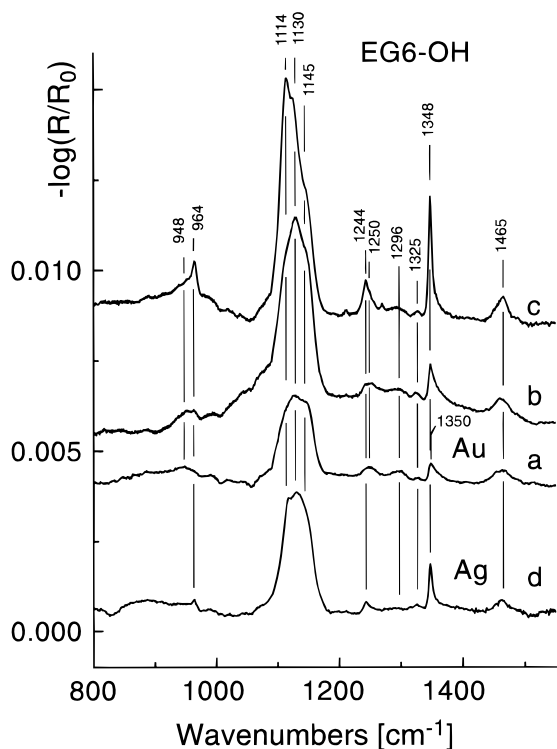


**Figure 2.** Detail IR spectra for four different EG6-OH samples on Au (a–c) and Ag (d) from a solution in ethanol. Spectra c and d show crystalline-like bandwidths and peak positions for the EG6 ether phase, whereas the spectra a and b show peak positions similar to amorphous-phase poly(ethylene glycol).

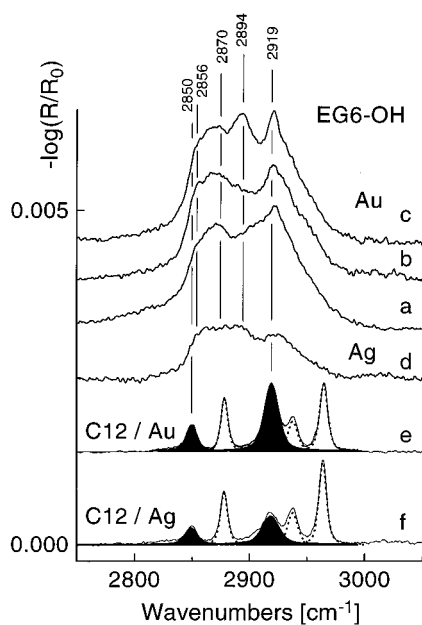


**Figure 3.** CH-stretching region of EG6-OH samples on Au (a–c) and Ag (d), respectively, in comparison with the spectrum of unfunctionalized dodecanethiolate ( $C_{12}$ ) on Au and Ag, for which the alkyl  $CH_2$ -stretching bands (bold lines) were deconvoluted with a peak-fitting routine from  $CH_3$ -stretching and Fermi resonance bands (dotted lines).

Spectrum 2a is similar to the transmission spectrum of the liquid compound in the range 800–1500  $cm^{-1}$ . The shoulder at the high-frequency side of the COC stretching band at ca. 1145  $cm^{-1}$  and the widths and positions of the ether  $CH_2$ -rocking (948  $cm^{-1}$ ), -twisting (1250 and 1296  $cm^{-1}$ ), and -wagging (1350  $cm^{-1}$ ) modes are all characteristic for amorphous poly-(ethylene glycol) with TGT, TGG, and GGT conformations.

This sample was not protein resistant, and we assume only an incomplete monolayer formed.

Spectrum 2b shows an increase of the  $CH_2$ -wagging mode at 1348  $cm^{-1}$ , characteristic for gauche conformations as in crystalline PEG, and an increase of the COC-stretching modes around 1130  $cm^{-1}$ . It thus presents a sample where both helical and amorphous EG moieties are present and is representative for the majority of the EG6-OH samples in this work. Spectrum 2c shows a further decrease in width and an increase in intensity and a shift for the rocking and twisting bands from amorphous-like band positions of 948 and 1250  $cm^{-1}$  to crystalline-like band positions of 964 and 1244  $cm^{-1}$ . Samples such as c that exhibited a high crystallinity in the polyether phase were exceptional (6 out of  $\sim 100$ ). The degree of crystallinity did not correlate to the immersion time or thiol concentrations used. The spectrum denoted as c corresponds to a sample from a 40  $\mu M$  solution with 10 min immersion time; other samples having a crystalline ether phase were immersed for 1–4 days in a 2 mM solution.

The spectrum 2d for EG6-OH on Ag is similar to the spectrum c for EG6-OH on Au and shows a mixture of bands that can be assigned to domains with an oriented crystalline helical phase (964, 1114, 1348  $cm^{-1}$ ) coexisting with a more amorphous phase (1145, 1325  $cm^{-1}$ ).

The orientation of the alkyl chains relative to the surface can be deduced from the relative intensities of their  $CH_2$ -stretching vibrations (Figure 3).<sup>33,34</sup> As a reference for the alkyl chain orientation in the EG6-OH films, we show the spectra of an unfunctionalized dodecanethiolate ( $C_{12}$ ) monolayer on Au (tilt angle with respect to the surface normal  $\sim 30^\circ$ ) and on Ag (tilt angle  $\sim 10^\circ$ ), in which the alkyl  $CH_2$ -stretching bands (bold lines) were deconvoluted.<sup>35</sup> Alkyl  $CH_3$ -stretching (2878, 2964  $cm^{-1}$ ) and the  $CH_3$ -Fermi resonance band (2938  $cm^{-1}$ ), which are not present in the spectra of the oligo(ethylene glycol)-terminated monolayers, are indicated by the dashed lines.

All EG6-OH spectra have in common that the relative intensities of the alkyl  $CH_2$ -stretching bands (Figure 3) at 2856  $cm^{-1}$  (shoulder) and 2921  $cm^{-1}$  are reduced compared to the isotropic EG6-OH transmission spectra shown in Figure 1, indicating a preferential orientation of the alkyl chains in the film. The similar intensity and peak position (within 1  $cm^{-1}$ ) of the asymmetric alkyl  $CH_2$ -stretching band for all three EG6-OH samples on Au (a–c) indicate that the orientation and conformation of the alkyl chains are not affected much by the phase transition in the EG6-OH ether phase. The asymmetric alkyl  $CH_2$ -stretching mode frequency of 2921  $cm^{-1}$  indicates that the  $C_{11}$ -alkyl phase has more gauche defects than the unfunctionalized  $C_{12}$ -thiol (2919  $cm^{-1}$ ), but fewer than in the liquid phase (2926  $cm^{-1}$ ). The symmetric alkyl  $CH_2$ -stretching mode frequency appears to be shifted by the underlying broad stretching mode of the OEG units. A symmetric ether  $CH_2$ -stretching band characteristic for gauche conformations is detected as a broad band with a maximum around 2870  $cm^{-1}$ . The strong band in the CH-stretching region at 2894  $cm^{-1}$  in spectrum c can be assigned to the symmetric  $CH_2$ -stretch of the crystalline helical EG6-OH units present in the film.<sup>36</sup>

For EG6-OH on Ag, the spectrum shows a reduced intensity of the alkyl  $CH_2$ -stretching modes and a simultaneous reduction of the spectral intensity of the OEG  $CH_2$ -stretching bands at 2870  $cm^{-1}$  and the shoulder around 2930  $cm^{-1}$  (characteristic for amorphous EG6-OH) as compared to Au. The similar reduction of the alkyl  $CH_2$ -stretching modes for unfunctionalized  $C_{12}$ -alkanethiolates and EG6-OH SAMs on Ag indicates that

**TABLE 1: Spectral Mode Assignments for PEG, EG6-OH, and EG3-OMe<sup>a</sup>**

mode assignment	PEG, crystal.	polarization    or $\perp$ to the helical axis	PEG, amorphous	EG6-OH/EG3-OMe liquid	EG6-OH/Au EG3-OMe/Au SAM
OH stretch				~3440 b/-	~3440 b
CH <sub>3</sub> asym. stretch				-/2980 sh	-/2982 s
EG CH <sub>2</sub> asym. stretch	2950	$\perp$	2930 sh		~2930 sh
alkyl CH <sub>2</sub> asym. stretch				2925 s	2921 s/2919 s
EG CH <sub>2</sub> sym. stretch	2890 s		2865 b		2870 b...2894 s
	2885 s	$\perp$			2870 b; 2896 s
	2865 sh				
alkyl CH <sub>2</sub> sym. stretch				2855 s	~2856 sh/~2853 sh
CH <sub>3</sub> sym. stretch				-/2820 sh	-/2819 s
combination vibration	2740		2740 sh	2740 sh/2740 sh	2740 w/2740 w
alkyl CH <sub>2</sub> scissor				1467 sh	1467 sh/1467 sh
EG CH <sub>2</sub> scissor (gauche)	1470 m	$\perp$	1460 m	1461 m	1463 m...1465 m
	1460 m				1461 m
EG CH <sub>2</sub> wag (gauche)	1345 s		1352 m	1351 m	1348 m...1348 s/1350 s
EG CH <sub>2</sub> wag (trans)			1325 w	1325 w	1325 w/1325 w
EG CH <sub>2</sub> twist	1283 m	$\perp$	1296 m	1298 m	1296 m/1297 m
EG CH <sub>2</sub> twist	1244 m		1249 m	1249 m/1247 m	1250 m...1244 s/1244 m
EG OCH <sub>3</sub> rocking				-/1199	-/1204
C-O, C-C stretch	1149 s	$\perp$	1140 sh		EG6-OH:
	1119 s	$\perp$			1130 s; 1145 sh
	1102 vs		1107 s	1113 s	...
	1062 m	$\perp$	1038 m		1114 vs; 1130 s; 1145 sh
					EG3-OMe:
					1136 s
EG CH <sub>2</sub> rocking (gauche)	963 s		945 m	948 m/944 m	948 m...964 s/960 m

<sup>a</sup> w weak, m medium, s strong, vs very strong, b broad, sh shoulder, asym asymmetric, sym symmetric. PEG: poly(ethylene glycol). EG6-OH: HS(CH<sub>2</sub>)<sub>11</sub>(OCH<sub>2</sub>CH<sub>2</sub>)<sub>6</sub>OH. EG3-OMe: HS(CH<sub>2</sub>)<sub>11</sub>(OCH<sub>2</sub>CH<sub>2</sub>)<sub>3</sub>OCH<sub>3</sub>.

the average tilt angle of the EG6-OH alkyl chains depends on the substrate lattice and not on the steric requirements of the OEG units.

In summary, a comparison to the C<sub>12</sub> spectra shows that the intensities of the symmetric and asymmetric alkyl CH<sub>2</sub>-stretching bands in the EG6-OH spectra on Au and Ag are roughly the same as in the C<sub>12</sub> spectra on the respective substrates and therefore indicate a similar cant angle. Table 1 summarizes the above band assignments.

**3.2.2. EG3-OMe and EG[3,1]-OMe on Gold and Silver Surfaces.** In contrast to the EG6-OH films, the EG3-OMe films on Au showed less variation from sample to sample. The EG3-OMe spectrum on Au, which is shown in Figure 4b, was the spectrum with the strongest and sharpest CH<sub>2</sub>-wagging, -twisting, and -rocking modes. Mode frequencies of 1350, 1244, and 960 cm<sup>-1</sup> are shifted from the amorphous-phase-like frequencies of the neat liquid of 1351, 1247, and 944 cm<sup>-1</sup> and indicate a predominantly helical conformation of the EG3 units. The spectrum also exhibits a shoulder at 1114 cm<sup>-1</sup> on the low-frequency side of the C-O-C-stretching band. This shoulder is also observed for the crystalline EG6-OH ether phase and crystalline PEG, where it is assigned to a C-O-C-stretching mode polarized parallel to the helical axis.<sup>36</sup> A preferential orientation parallel to the surface normal can also be derived from the relative strength of the crystalline-like, parallel-polarized, twisting mode at 1244 cm<sup>-1</sup> and the absence of the twisting band for the crystalline phase at 1283 cm<sup>-1</sup> with perpendicular polarization.

The spectrum for EG3-OMe on Ag (Figure 4a) shows a single, sharp, strong C-O-C-stretching mode at 1145 cm<sup>-1</sup>, but no gauche CH<sub>2</sub>-CH<sub>2</sub>-wagging band at 1350 cm<sup>-1</sup>. The band at 1325 cm<sup>-1</sup> is assigned to the wagging mode of glycol units with a C-C trans conformation. This band assignment is strictly valid only for isolated C-C trans conformations in the amorphous phase. For planar oligomers with more than one C-C trans conformation, the individual CH<sub>2</sub>-CH<sub>2</sub> trans wagging modes will couple and split into a series of modes

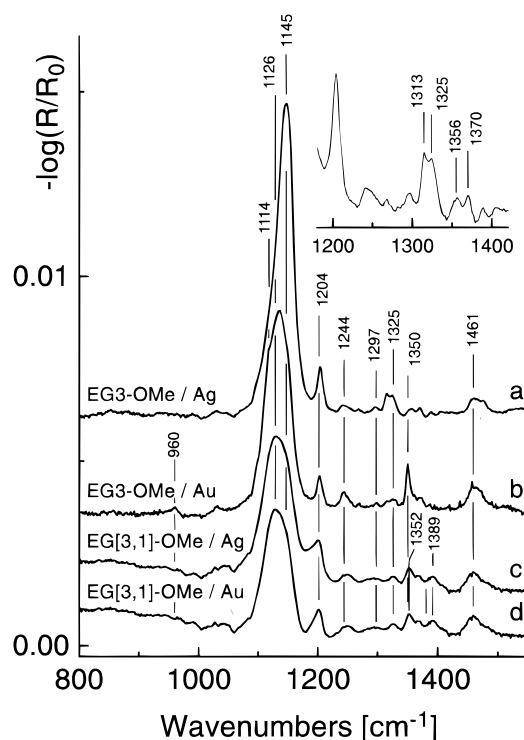


**Figure 4.** IR spectral region from 800 to 1550 cm<sup>-1</sup> for EG3-OMe and EG[3,1]-OMe samples on Au and Ag. The enlarged detail spectrum of EG3-OMe on Ag shows a CH<sub>2</sub>-wagging mode at 1325 cm<sup>-1</sup> that can be assigned to the C-C trans conformation, but no other CH<sub>2</sub>-wagging mode at 1352 cm<sup>-1</sup> that would indicate a C-C gauche conformation.

with different phases, intensities, and frequencies. The band at 1313 cm<sup>-1</sup>, which does not appear in the spectra of EG3-OMe on Au, might be attributed to such coupled wagging modes (see inset in Figure 4). The shift of the COC-stretching vibration from 1130 cm<sup>-1</sup> for EG3-OMe on Au to 1145 cm<sup>-1</sup> on Ag is also indicative of conformational changes in the OEG moiety.

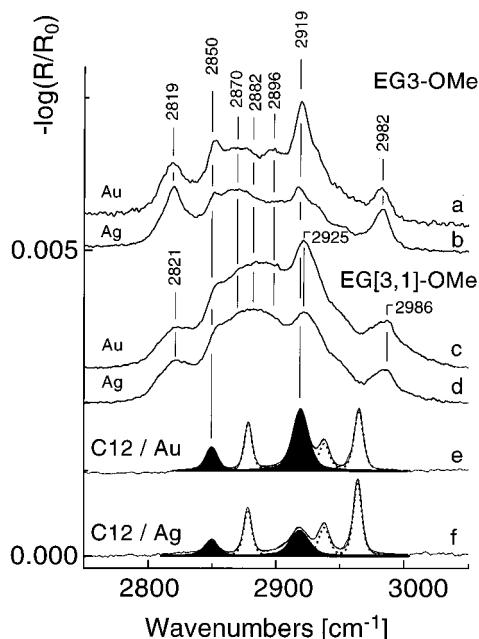


**Figure 5.** CH-stretching region of EG3-OMe, EG[3,1]-OMe, and dodecanethiolate (C<sub>12</sub>) on Au and Ag (a–d). In e and f, the CH<sub>2</sub>-stretching bands (bold lines) were deconvoluted with a peak-fitting routine from CH<sub>3</sub>-stretching and CH<sub>3</sub>-Fermi resonance bands (dotted lines).

The symmetric C–O–C peak shape corresponds neither to the broad, asymmetric peak<sup>37</sup> in amorphous PEG nor to the sharp multiplet for crystalline PEG.<sup>38</sup>

EG[3,1]-OMe samples on Au (Figure 4d) show an amorphous-like C–O–C-stretching mode at 1126 cm<sup>-1</sup> and broadened wagging, twisting, and rocking modes typical for the liquid state. The conformation around the ether C–C bonds is predominantly gauche, as indicated by the wagging mode at 1352 cm<sup>-1</sup>. The same applies to EG[3,1]-OMe samples on Ag (Figure 4c).

The intensities of the EG3-OMe alkyl CH<sub>2</sub>-stretching modes (Figure 5a) on Au are similar to the intensities of C<sub>12</sub> and EG6-OH SAMs, indicative of an alkanethiolate phase with a similar cant angle. For EG3-OMe on Ag the very low intensity of the ether and alkyl CH<sub>2</sub>-stretching vibrations (Figure 5b) and the high packing density determined by XPS (see below) imply a smaller tilt angle of the alkyl chains and that the planar ethylene glycol units are oriented nearly parallel to the surface normal. For comparison, we also display the respective C<sub>12</sub> alkanethiolate spectra on Au and Ag (Figure 5e,f). The asymmetric alkyl CH<sub>2</sub>-stretching mode frequencies at 2917 cm<sup>-1</sup> on Ag and 2919 cm<sup>-1</sup> on Au for EG3-OMe are the same as for the unfunctionalized alkanethiolates and indicate a similar low density of gauche defects in the alkyl phase. The alkyl CH<sub>2</sub> stretching mode is at a lower frequency for EG3-OMe on silver than for EG3-OMe on gold and indicates a higher degree of crystallinity in the alkane phase.

The spectral intensities for the EG3-OMe CH<sub>3</sub>-stretching bands at 2820 and 2980 cm<sup>-1</sup> on Ag are about the same as the data for EG3-OMe on Au. The intensity ratios between the symmetric and asymmetric stretching mode are the same for Au and Ag and thus indicate the same average orientation of the terminal methoxy group. This is in agreement with the results for methoxy-terminated alkanethiolates, where the same spectral characteristics for the terminal methoxy group were observed on Au and Ag,<sup>39</sup> suggesting that the orientation of the terminal methoxy group is decoupled from the alkyl chain cant angle.

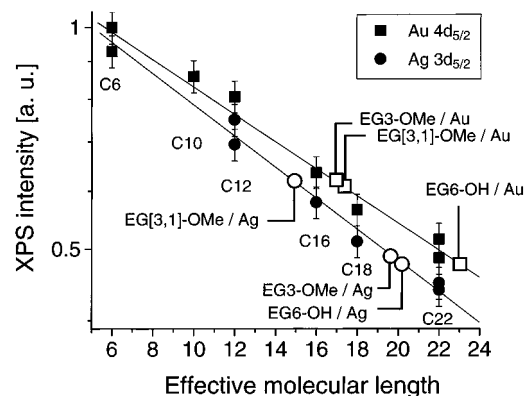


**Figure 6.** Attenuation of the substrate photoelectron intensity for unsubstituted alkanethiolates with 6, 10, 12, 16, 18, and 22 carbon atoms. The logarithmic Ag 3d<sub>5/2</sub> and Au 4d<sub>5/2</sub> intensities decrease linearly with increasing molecular length and the least-squares fit for unfunctionalized SAMs can be used as a reference to determine the effective thicknesses of oligo(ethylene glycol)-terminated SAMs. The indicated thicknesses do not include the sulfur atom layer, which corresponds to  $\sim 1.5$  molecular length units (carbon or oxygen atoms).

The EG[3,1]-OMe alkyl CH<sub>2</sub>-stretching band intensities are less distinct on Au and Ag than in the case of EG6-OH or EG3-OMe. For both EG[3,1]-OMe samples on Au and Ag, the asymmetric CH<sub>2</sub>-stretching mode maximum is shifted to a liquidlike frequency 2925 cm<sup>-1</sup>, suggesting that the alkyl chains are disordered by the steric requirements of the branched end group. The two different –OCH<sub>3</sub> end groups in EG[3,1]-OMe give broad symmetric and asymmetric CH<sub>3</sub>-stretching modes at  $\sim 2821$  cm and  $\sim 2986$  cm<sup>-1</sup>.

**3.3. X-ray Photoelectron Spectroscopy (XPS).** XP spectroscopy gives information about the stoichiometry and thickness of the films on Au and Ag. Assuming a homogeneous adsorbate layer, we estimated the film thickness  $d$  from the attenuation of substrate photoelectrons (Au 4d and Ag 3d), which decrease exponentially with increasing adsorbate thickness. We used a reference system of six alkanethiolates (C<sub>6</sub>–C<sub>22</sub>) on Au and four<sup>40</sup> alkanethiolates on Ag (C<sub>12</sub>–C<sub>22</sub>) with 6, 10, 12, 16, 18, or 22 carbon atoms (Figure 6) to determine the relative thickness of the OEG-terminated SAMs. We assumed that the six  $n$ -alkanethiolates have the same average alkyl chain tilt angle of 30° on Au and  $\sim 10^\circ$  on Ag to calculate the effective thickness of the oligo(ethylene glycol)-terminated SAMs (using a value of 1.26 Å per methylene unit). Linear regression of the data gave attenuation lengths<sup>41</sup> of 26 Å for both the Au 4d<sub>5/2</sub> and the Ag 3d<sub>5/2</sub> photoelectrons.<sup>42</sup> These results are somewhat lower than the interpolated values of 29–34 Å for Au 4d<sub>5/2</sub> or Ag 3d<sub>5/2</sub> electrons attenuated by  $n$ -paraffins, polyethylene,<sup>43</sup> and alkanethiolates<sup>44</sup> using empirical best fit expressions such as the TPP-2M equation<sup>45</sup> or the  $\lambda \propto E_{\text{kin}}^{0.67}$  expression found by Laibinis et al.<sup>46</sup> However, the attenuation length depends on the extent of elastic scattering, which is a function of electron emission angle and incidence angle of the X-rays.<sup>47</sup> The somewhat lower value of  $\lambda$  derived from our measurements at near-normal emission angle as compared to previous measurements<sup>44,46</sup> at grazing emission angles is in agreement with theoretical predictions.<sup>47</sup>

The experimental data (Figure 6) reveal that the attenuation of the Au 4d substrate photoelectrons by an EG6-OH film with 23 methylene groups and 7 oxygen atoms corresponds to the attenuation by an unsubstituted C<sub>23</sub> SAM.<sup>48</sup> On Ag, the attenuation corresponds to a C<sub>20</sub> SAM. These values correspond to 78% and 68% of the theoretical thickness<sup>49</sup> on Au and Ag, respectively.

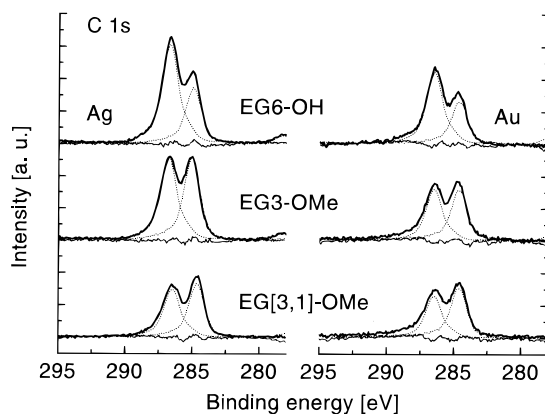


**Figure 7.** XPS C 1s spectra of EG6-OH, EG3-OMe, and EG[3,1]-OMe on Au and Ag. The C 1s spectral envelopes were deconvoluted in an ether C 1s peak at 286.7 eV and an alkyl C 1s peak at 284.9 eV.

For EG3-OMe, the attenuations of the substrate photoelectrons roughly correspond to the predicted attenuation by a C<sub>17</sub> (Au) and C<sub>19</sub> (Ag) alkanethiolate monolayer. EG3-OMe consists of 22 ether oxygen and methyl(ene) units, and the effective thickness is 79% of the theoretical value on Au and 85% on Ag. On Ag, the surface coverage of the alkanethiolates is higher and the molecular cross section is smaller than on Au.

For EG6-OH on Ag, the IR data suggest a helical conformation of the EG6-OH group and a less tilted alkyl chain than on Au. The unit cell area of unfunctionalized alkanethiolates on Ag<sup>50</sup> is  $\sim 10\%$  smaller than the molecular cross section of a helical -EG6-OH group (19.1 Å<sup>2</sup> as compared to 21.3 Å<sup>2</sup>, see the discussion). This difference requires the presence of voids or defects in the alkyl phase to accommodate the helical conformation and therefore results in a similar calculated surface coverage as on gold.

EG3-OMe monolayers show a higher surface coverage on Ag than on Au. The effective film thickness is  $\geq 85\%$  of the predicted value for a monolayer of densely packed EG3-OMe chains with an orientation close to perpendicular to the surface plane. IR data show that EG3-OMe on Ag does not adopt the helical conformation, inferring that the surface packing density is too high to allow a helical conformation of the ethylene glycol units.

In EG[3,1]-OMe SAMs, the -CH<sub>2</sub>-O-CH<sub>3</sub> side chain is expected to reduce lateral packing density and effective thickness in comparison with EG3-OMe. The experimentally determined effective molecular lengths of 17.5 for EG[3,1]-OMe on Au and 15.5 on Ag are roughly the same (Au) or lower (Ag) than for EG3-OMe.

The carbon atoms of the alkyl chain and the ether carbon atoms can be distinguished by their distinct C 1s peaks at 284.9 and 286.8 eV, respectively (Figure 7). To verify the bilayer structure of the SAMs, we deconvoluted the C 1s doublet into the alkyl and polyether fraction by a numerical least-squares routine using the normalized C 1s spectrum of PEG 8000 for the polyether phase and the spectrum of a dodecanethiolate SAM as a reference for the alkyl C 1s peak. If the SAMs adopt an oriented structure, the OEG moieties will attenuate the intensity of the underlying alkyl carbon atoms and produce a ratio of the polyether carbon C 1s to the alkyl carbon C 1s peak above the values expected from the stoichiometric ratios of 1.3 (13/10) for EG6-OH, 0.8 (8/10) for EG3-OMe, and 0.83 (10/12) for EG[3,1]-OMe.

The deconvolution of the C 1s peak gives ratios for the C 1s ether to the C 1s alkyl intensities on Au and Ag of 1.62 and 1.89 for EG6-OH, 0.96 and 1.11 for EG3-OMe, and 0.81 and 0.95 for EG[3,1]-OMe, respectively (Table 2). With the exception of EG[3,1]-OMe on Au, the values are significantly higher than the corresponding stoichiometric ratios, indicating attenuation of the alkyl C 1s emission and thus supporting the model of a layered structure.

For SAMs with a layered structure of alkyl and polyether phases with thickness  $d_{\text{OEG}}$ , the C 1s signal from the alkyl methylene units should be attenuated by  $\exp(-d_{\text{OEG}}/\lambda_{\text{C 1s}})$ , and the C 1s signal of the  $i$ th of  $n$  polyether carbon atoms should be attenuated by the overlying  $n-i$  carbon and their adjoining oxygen atoms.<sup>51</sup> We assumed a value of 27 Å for  $\lambda_{\text{C 1s}}$ , close to the value of  $\lambda$  for Ag 3d<sub>5/2</sub> estimated for our experimental conditions from the data in Figure 6. For such an ideal EG6-OH bilayer with helical polyether phase, we calculate a C 1s alkyl/C 1s ether ratio of 1.85, close to the experimental value of 1.89 for EG6-OH on Ag. The corresponding ratio for EG3-OMe is 1.01 for a helical ether phase and 1.08 for a planar EG conformation. The experimental data agree within  $\pm 5\%$  of the predicted values for an ideal bilayer structure.

From the XPS data, we therefore conclude that the films are not perfectly homogeneous, as assumed for the theoretical estimates; they contain defects and/or domain boundaries resulting in a lower effective thickness. The bilayer model describes the experimental results for EG6-OH and EG3-OMe well on a silver substrate, whereas the deviation of the model predictions for the two molecules on Au, and for EG[3,1]-OMe on both substrates, indicates a higher degree of disorder.

**3.4. Fibrinogen Adsorption Experiments.** Fibrinogen was used as a model protein for measuring the protein resistance of OEG-terminated SAMs, because adsorption experiments on various surfaces with single protein solutions of albumin, IgG, and fibrinogen (the three main components of blood plasma)

**TABLE 2: Effective Film Thicknesses for EG6-OH, EG3-OMe, and EG[3,1]-OMe SAMs on Au and Ag**

		$d_{\text{calc}} [\text{Å}]^a$		$d_{\text{exp}} [\text{Å}]^a$	C 1s ether:C 1s alkyl	
		helical	planar		calc <sup>b</sup>	exptl
Au	EG6-OH	30.8		25	1.30–1.85 (helical)	1.62:1
Au	EG3-OMe	23.3		20	0.80–1.01 (helical)	0.96:1
Au	EG[3,1]-OMe			21	>0.83	0.81:1
Ag	EG6-OH	30.8	37.5	26	1.30–1.85 (helical)	1.89:1
Ag	EG3-OMe	23.3	28.3	26	0.80–1.08 (planar)	1.11:1
Ag	EG[3,1]-OMe			21	>0.83	0.95:1

<sup>a</sup> The relative molecular lengths as indicated in Figure 6 were multiplied by the incremental length per methylene unit for a perpendicular oriented alkyl chain (Ag) of 1.26 and 1.1 Å for an all-trans chain tilted by 30° from the surface normal (Au) plus the length of the C–S bond. Theoretical thicknesses for the oligo(ethylene glycol) end groups were predicted from the incremental thicknesses of 2.78 Å for the helical conformation and 3.56 Å for the planar conformation. <sup>b</sup> The lower value is the stoichiometric ether carbon:alkyl carbon atoms ratio; the higher value corresponds to an ideal bilayer structure, where the alkyl carbon C 1s intensity is attenuated by the overlying OEG strands with helical (EG6-OH on Au, Ag; EG3-OMe on Au) or planar (EG3-OMe on Ag) conformation.

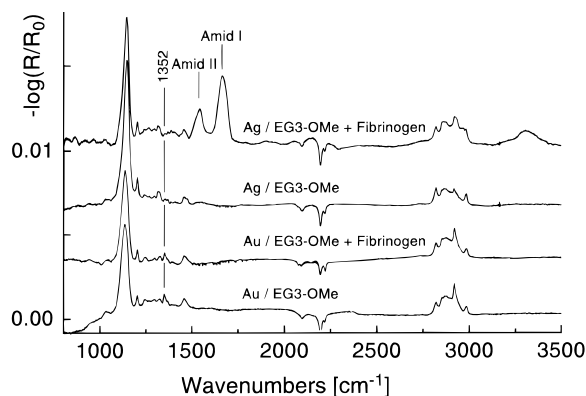


**Figure 8.** EG3-OMe SAMs before and after immersion in fibrinogen solution. EG3-OMe on Ag is not protein resistant like EG3-OMe on Au but adsorbs up to 60% of a monolayer fibrinogen as determined by the intensities of the amide I and amide II bands of the fibrinogen film.

showed a maximum surface coverage for fibrinogen.<sup>52</sup> Also, competitive adsorption experiments from ternary albumin–IgG–fibrinogen solutions revealed a preference for fibrinogen.<sup>10</sup>

Experiments with EG6-OH and EG[3,1]-OMe SAMs on Au and Ag, both for the more densely packed helical phase of EG6-OH and the predominantly amorphous ether phase for the two molecules, showed that these films were completely resistant to protein adsorption if the adsorption time was sufficient for the formation of a monolayer film. On incomplete films of EG6-OH and EG3-OMe with an immersion time of 1 min, ca. 40% of a monolayer of fibrinogen adsorbed. The amount of protein adsorption was much lower for more complete SAMs, and 30 min immersion times for formation of the SAMs were found to be sufficient to form an intact film. The representative FTIR data for the protein resistant EG6-OH films are shown in Figure 2. These findings agree with earlier results.<sup>10</sup>

Our FTIR data showed that adsorption of EG3-OMe on Au and Ag resulted in different preferential molecular conformations of the OEG moiety: on gold, the ethylene glycol units were observed to be predominantly in their room-temperature helical gauche conformation, whereas on silver we found that the majority of the oligo(ethylene glycol) units assumed the planar “all-trans” conformation. In the fibrinogen adsorption experiments, we observed that films on silver exhibiting predominantly the all-trans phase (no C–C gauche wagging mode at 1352  $\text{cm}^{-1}$  detectable) adsorbed fibrinogen in a range of 5%–60% of a monolayer (Figure 8a,b), whereas the EG3-OMe films with gauche conformations on gold were consistently protein resistant (Figure 8c,d). The highest amounts of protein adsorption on Ag/EG3-OMe were observed when the C–O–C-stretching band maximum was observed at 1145  $\text{cm}^{-1}$  before and after immersion in the buffered, aqueous fibrinogen solution. The lower limit for the amount of protein adsorption (5%–10%) corresponds to EG3-OMe samples which showed some relaxation of the ether phase during exposure to the fibrinogen solution, indicated by a shift of the C–O–C band maxima to  $\sim 1140$   $\text{cm}^{-1}$ . Hence, for a densely packed film of EG3-OMe, the ability to resist fibrinogen adsorption correlates with molecular conformation. Analogous experiments with different OEG conformations in EG6-OH-terminated SAMs were not possible, because the helical conformation formed on both gold and silver surfaces.

#### 4. Discussion

**4.1. The Conformation of OEG on Au and Ag Surfaces.** We would first like to summarize and discuss our results relating

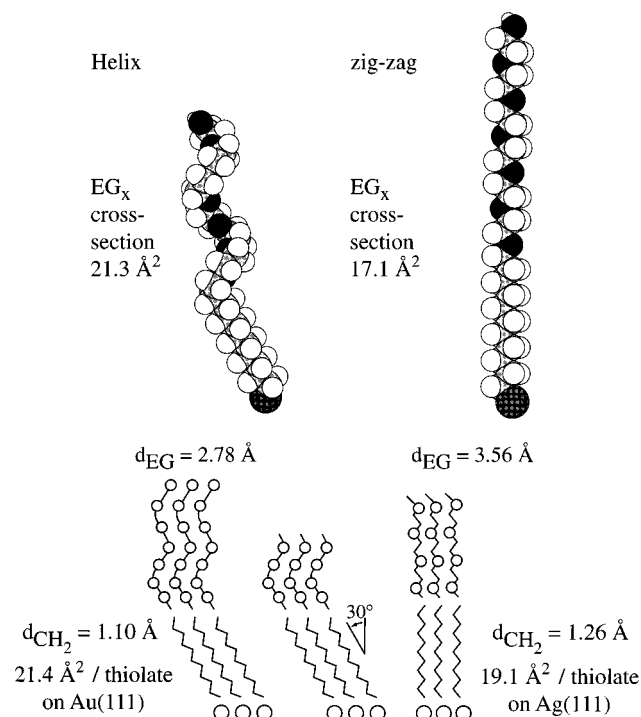


**Figure 9.** Molecular cross sections and incremental thickness per methylene and EG (–OCH<sub>2</sub>CH<sub>2</sub>–) unit, respectively, for EG6-OH on Au with a  $\sim 30^\circ$  tilt of the alkyl chain and a perpendicular orientation of the EG6 helix axis and for EG3-OMe with a perpendicular orientation of the alkyl chain and a planar zigzag conformation of the EG units.

to the different molecular conformations observed for the OEG moieties in the self-assembled monolayers. Neat EG6-OH, EG3-OMe, and EG[3,1]-OMe are liquids at room temperature, whereas EG $n$ -OH oligo(ethylene glycol) amphiphiles with a dodecyl chain and  $n > 6$  are crystalline solids at room temperature.<sup>53</sup> In the liquid or amorphous state, no preferred molecular conformation is observed: The conformation of the C–C bond is mainly gauche, but without uniform rotation, and the conformation around the C–O bond can be trans or gauche.

In a SAM, the anchoring of  $n$ -alkanethiols to the Au and Ag surfaces favors a parallel alignment of the alkyl chains and a crystalline-like all-trans conformation for  $n > 10$ .<sup>12</sup> Like the dodecyl oligo(ethylene glycol) series,<sup>40</sup> the ordered arrangements of the oligo(ethylene glycol)-terminated alkanethiols should favor a helical conformation of the OEG moieties if they are not spatially restricted.

In the following discussion, we assume that our polycrystalline Au and Ag surfaces consist predominantly of (111) facets in order to relate our observations to the structural data available for alkanethiols on defined gold and silver surfaces. Figure 9 summarizes an idealized model for the adsorption geometries and conformations for EG6-OH and EG3-OMe on Au(111) and Ag(111). The sulfur atoms of unfunctionalized long-chain alkanethiols on Au(111) form a commensurate hexagonal ( $\sqrt{3} \times \sqrt{3}$ )R30° overlayer<sup>54</sup> with an S···S spacing of 4.97 Å and an idealized (for a defect-free film) packing density of 21.4 Å<sup>2</sup>/thiolate. To optimize the van der Waals contact, the alkyl chains must tilt from the surface normal by  $\sim 30^\circ$  as observed by IR<sup>15</sup> spectroscopy and grazing incidence X-ray diffraction.<sup>55</sup> The resulting alkyl chain density and cross sectional area perpendicular to the chain axis are the same as for polyethylene (18.4 Å<sup>2</sup>). Crystalline poly(ethylene glycol) in its idealized helical form has a larger molecular cross section of 21.3 Å<sup>2</sup>, but can be accommodated on top of the crystalline polyethylene layer with an in-plane packing density of 21.4 Å<sup>2</sup>/thiolate

molecule. Due to lateral constraints in the densely packed phase, the oligo(ethylene glycol) moieties adopt an orientation parallel to the surface normal and attain their bulk mass density.

On Ag(111), the S··S spacing for long-chain alkanethiols is smaller ( $4.77 \pm 0.03 \text{ \AA}$ )<sup>50</sup> than on Au(111). The molecules assume a more perpendicular orientation with respect to the surface plane, and the surface area per molecule ( $18.4 \text{ \AA}^2$ ) is nearly the molecular cross section of the alkyl chains. The smaller domain size of the alkanethiolates and the presence of defect sites<sup>56</sup> on Ag(111) cause average molecular tilt angles of  $7\text{--}14^\circ$ .<sup>57</sup> Since the molecular cross section of helical poly(ethylene glycol) is larger than the unit cell dimension of unfunctionalized alkanethiols on Ag(111), the helical form cannot easily be accommodated. That the EG6-OH molecules are adsorbed in their energetically more favorable helical conformation on Ag(111) indicates that the EG6-OH film must have vacancies or defects and/or that the underlying alkane lattice is expanded as compared to neat alkanethiolates. For the EG3-OMe films, the energetic advantage of the helical form versus the all-trans form of the OEG units is smaller<sup>58</sup> than for EG6-OH, so that the tri(ethylene glycol) unit more easily adopts a planar zigzag conformation with a cross section of  $17.1 \text{ \AA}^2$ , which can be accommodated in the alkanethiolate lattice on Ag(111).

The different film densities for EG6-OH and EG3-OMe on silver are also evident in the XPS data, where we found that the film thicknesses (as measured by the attenuation of the substrate signal) are about the same despite their different molecular lengths. This observation confirms that the lateral density in the two films are different on silver surfaces, as suggested above.

These observations indicate that the energy differences are small and that a subtle balance between the headgroup/substrate energetics, alkane/alkane chain interactions, and the energy differences between the conformations of the OEG moiety determine the phase behavior and molecular conformation in the OEG SAMs. To our knowledge, this is the first example where the conformation of the tailgroup of an  $\omega$ -terminated monolayer can be tuned by the choice of the substrate material.

The deviation of the idealized model from the experimental observation, i.e., the presence of amorphous conformations in the predominantly helical or all-trans OEG phase (in the FTIR data) and the lower than expected absolute film thickness (derived from XPS), is not unexpected considering the polycrystalline nature of the substrates and the well-documented presence of domain boundaries due to the canted orientation of the molecules in the alkanethiolate films.

The bulky nature of the EG[3,1]-OMe molecules obviously prevents the formation of an oriented and well-ordered film. The FTIR data show that the alkyl chains for this molecule are less ordered than in simple alkanethiolate films and that the OEG moieties are best described by an amorphous conformation. Accordingly, these films are less dense than the EG6-OH and EG3-OMe films, as confirmed by the XPS data.

**4.2. Protein Resistance of the Films.** That the helical and the amorphous-like OEG phases in the EG6-OH and EG3-OMe films and the less densely packed EG[3,1]-OMe samples are protein resistant is consistent with previous results. Whitesides et al.<sup>10,59</sup> reported not only that the pure EG6-OH films resist protein adsorption but also that resistance was maintained in mixed layers of EG6-OH with *n*-alkanethiols as long as the mole fraction of the latter did not exceed  $\sim 35\%$ . On the basis of the measurements described here, we expect that the OEG strands in these diluted EG6-OH SAMs have amorphous conformations.

It is noteworthy, however, that the densely packed and crystalline-like helical OEG-terminated SAMs are also protein resistant. These films do not present a long-range steric barrier to the proteins,<sup>60</sup> and their observed protein resistance is consistent with the notion that the surface film prevents adsorption onto the substrate simply by preventing the protein from reaching the interface.<sup>61</sup> The crystalline-like, ordered EG6-OH samples in our measurements are completely fibrinogen resistant. This result agrees with the theoretical work of Szleifer,<sup>60</sup> who found that the presence of *flexible* poly(ethylene glycol) strands is not a necessary condition for protein resistance, but rather a dense and inert film that prevents contact between the substrate and the protein.

The question then remains, why the protein does not adsorb onto the EG3-OMe SAM surface, which is substantially less hydrophilic than  $-\text{OH}$ -terminated alkanethiolates. To explain this observation, it is significant that the predominantly *helical* EG3-OMe films on Au are protein resistant, whereas the EG3-OMe layers which are densely packed and mainly in a trans conformation on Ag do adsorb protein. The distinction between the two conformations can be made by the characteristic vibrations in the FTIR data; they cannot be distinguished by different contact angles of water. The observation of identical (within the errors of measurement) wettabilities is in agreement with the FTIR data (Figure 5), where the orientation of the terminal  $\text{CH}_3$  group is found to be the same, which suggests that the wetting properties might also be similar. Obviously, the water contact angle measurements taken in air are not sensitive to the molecular conformation of the OEG moieties, or the differences in the molecular conformation inferred from the nitrogen-purged FTIR experiments disappear in the presence of liquid water.

Despite the similarity in wettability by water droplets, the resistance to protein adsorption is significantly different for SAMs that have OEG units predominantly in the helical and planar trans conformations. In those EG3-OMe samples on Ag, where only a small amount of fibrinogen adsorption was detected, we observed a change in the IR absorptions of the OEG moieties, suggesting a transfer of molecules from the predominantly planar trans to the amorphous phase on adsorption of proteins. In other words, interaction with the protein-containing buffer solution or direct interaction with the protein changed the conformation of the EG3-OMe moieties. This observation suggests that protein resistance in these films is influenced by the molecular conformation of the OEG units in the interphase and not just by surface energy as determined by the orientation of the terminal functionality and probed by the contact angle of water on the neat films.

The helical, protein resistant conformation we observe in our FTIR spectra taken in a nitrogen atmosphere corresponds to the stable solvated form of the polymer at room temperature; desolvation at higher temperatures leads to an amorphous phase having a substantial population of trans conformations around the C–C bond.<sup>9</sup> Due to its high flexibility, the polymer does not assume a homogeneous all-trans conformation in its dehydrated, high-temperature, amorphous form, and therefore no experimental information on such a phase to compare with our data for EG3-OMe on Ag is available.

Correlating the molecular conformations of the OEG moieties with their ability to bind water, we speculate that the protein reaching the interface of the OEG-terminated SAMs by diffusion distinguishes whether it approaches a solvated or a partly desolvated interphase and that this affects its ability to bind irreversibly. If the water is strongly bonded and provides a

stable solvation shell, the protein might not be able to displace the bound water and, hence, to adsorb. In other words, the protein resistance of the helical OEG phase may not be a property of the molecule itself; instead, the helical phase may prevent a direct interaction between the surface and the protein by forming a stable solid-liquid interphase involving tightly bound water. This model is supported by quantum mechanical calculations on the solvation of the different OEG conformations,<sup>62</sup> which suggest that the all-trans phase of an OEG-terminated SAM cannot form a stable solvation layer, while the helical structure (due to its strong and self-perpetuating dipole field) stabilizes such a layer.

Note, however, that this model remains speculative as long there are no direct "in situ" experimental data establishing the molecular interaction of OEG in different conformations with water. The lack of a direct correlation of conformation with macroscopic wetting properties, as measured by the contact angle of water, is not obviously compatible with the hypothesis that the strength of interaction with water is the characteristic that determines protein adsorption, and requires further study. At this time, fibrinogen adsorption is a more sensitive probe of the interfacial properties of OEG-terminated alkanethiolate films than water contact angle measurements.

### Summary and Conclusions

FTIR and XP spectroscopies revealed that EG6-OH-, EG3-OMe-, and EG[3,1]-OMe-terminated SAMs on polycrystalline gold surfaces vary in their lateral density and in the molecular conformation of the OEG group. The EG6-OH films on Au show a high degree of variability in conformation and may exist in conformations ranging from a predominantly crystalline, helical phase to an amorphous phase characteristic of OEG conformations in the liquid state. Less variation of the film properties was observed for EG3-OMe-terminated SAMs. For EG[3,1]-OMe SAMs, the coverages measured by XPS and the FTIR data indicate a highly disordered alkanethiolate monolayer.

The conformation of the EG3-OMe-terminated alkanethiolate film can be manipulated by the choice of the substrate metal, i.e., gold or silver. On the former, the lateral spacing of the canted alkane chains allows the OEG units to accommodate their helical conformation. On silver, the alkane chains are oriented nearly perpendicular to the surface plane and the higher lateral density causes the methoxy-terminated tri(ethylene glycol) unit to assume trans conformations around their C-O bonds. To our knowledge, this example is the first where the molecular conformation in the tailgroup of an  $\omega$ -functionalized SAM can be manipulated by the choice of the substrate material.

Whereas the SAMs exhibiting the characteristic FTIR spectra of OEG moieties with helical or amorphous conformations were found to be resistant to fibrinogen adsorption, the dense EG3-OMe films on silver with OEG strands in a preferential "all-trans" conformation adsorb fibrinogen. The observation that dense and predominantly helical (but not defect-free) films of OEG-terminated SAMs are protein resistant suggests that conformational freedom (as present in grafted PEG coatings) is not a necessary condition for rendering the surface resistant to protein adsorption. We speculate that the conformation-dependent degree of solvation, and consequently the stability of an interfacial water layer, determines if the protein, reaching the surface by diffusion, can irreversibly adsorb onto the surface.

**Acknowledgment.** M.G. thanks the Deutsche Forschungsgemeinschaft and the DAAD for financial support of a sabbatical leave during which this work was initiated and completed, and

Harvard University for its outstanding hospitality. The substituted alkanethiols were synthesized by R. Bird (Harvard). The experimental work in Heidelberg was supported by the DFG, the work at Harvard University by the National Institutes of Health (GM 30367), and that at MIT by the Office of Naval Research, respectively.

### References and Notes

- (1) Harris, J. M., Ed. *Poly(ethyleneglycol) chemistry: biotechnical and biomedical applications*; Plenum Press: New York, 1992.
- (2) Bailey, F. E., Jr.; Koleske, J. Y. *Poly(Ethylene Oxide)*; Academic Press: New York, 1976.
- (3) PEGs are also sometimes referred to as poly(ethylene oxide) (PEO) and poly(oxyethylene) (POE). In this paper, the term poly(ethylene glycol) will be used for polymers of all molecular weights.
- (4) Lee, J. H.; Kopecek, J.; Andrade, J. D. *J. Biomed. Mater. Res.* **1989**, *23* (3), 351-368.
- (5) de Gennes, P. G. *Ann. Chim.* **1987**, *77*, 389. Taunton, H. J.; Toprakcioglu, C.; Fetters, L. J.; Klein, J. *Nature* **1988**, *332*, 712-714.
- (6) Jeon, S. I.; Lee, J. H.; Andrade, J. D.; de Gennes, P. G. *J. Colloid Interface Sci.* **1991**, *142*, 149-158.
- (7) Jeon, S. I.; Andrade, J. D. *Ibid.* **1991**, *142*, 159-166.
- (8) Gölander, C. G.; Herron, J. N.; Lim, K.; Claesson, P.; Stenius, P.; Andrade, J. D. In *Poly(ethyleneglykol) chemistry: biotechnical and biomedical applications*; Harris, J. M., Ed.; Plenum Press: New York, 1992; pp 221-245.
- (9) Lüsse, S.; Arnold, K. *Macromolecules* **1996**, *29*, 4251-4257.
- (10) Prime, K. L.; Whitesides, G. M. *J. Am. Chem. Soc.* **1993**, *115*, 10714-10721.
- (11) Wang, R. L. C.; Kreuzer, H. J.; Grunze, M. *J. Phys. Chem.* **1997**, *101*, 9767-9773.
- (12) Bain, C. D.; Troughton, E. B.; Tao, Y.-T.; Evall, J.; Whitesides, G. M.; Nuzzo, R. G. *J. Am. Chem. Soc.* **1989**, *111*, 321-335.
- (13) Pale-Grosdemange, C.; Simon, E. S.; Prime, K. L.; Whitesides G. M. *J. Am. Chem. Soc.* **1991**, *113*, 12-20.
- (14) Bird, R.; Mrksich, M.; Whitesides, G. M. Manuscript in preparation.
- (15) Laibinis, P. E.; Whitesides, G. M.; Allara, D. L.; Tao, Y.-T.; Parikh, A. N.; Nuzzo, R. G. *J. Am. Chem. Soc.* **1991**, *113*, 7152-7167.
- (16) Long-chain alkanethiols have low solubilities in hexane. Oligo-(ethylene glycol)-terminated alkanethiols are less soluble in hexane and showed a better ordering when prepared from ethanol as compared to hexane solution.
- (17) We observed that oligo(ethylene glycol)-terminated SAMs after removal from the solution decompose in the dark in air at 45 °C within a week. XP spectra showed a loss of ethylene glycol units and an oxidation of the thiol headgroup. At 20 °C, first signs of degradation were visible after storage in air longer than about 1 month. Storage of the samples in daylight did not enhance the decomposition rate.
- (18) Ulman, A. *An introduction to ultrathin organic films*; Academic Press: London, 1991.
- (19) Allara, D. L.; Swalen, J. D. *J. Phys. Chem.* **1982**, *86*, 2700-2704.
- (20) Takahashi, Y.; Tadokoro, H. *Macromolecules* **1973**, *6*, 672-675.
- (21) Matsuura, H.; Miyazawa, T. *J. Polym. Sci., Part A-2* **1969**, *7*, 1735-1744.
- (22) Liedberg, B.; Ivarsson, B.; Lundström, I. *J. Biochem. Biophys. Meth.* **1984**, *9*, 233-243.
- (23) Stenberg, E.; Persson, B.; Roos, H.; Urbaniczky, C. *J. Colloid Interface Sci.* **1991**, *143*, 513-526.
- (24) Engquist, I.; Lundström, I.; Liedberg, B. *J. Phys. Chem.* **1995**, *99*, 12257-12267.
- (25) Laibinis, P. E.; Bain, C. D.; Nuzzo, R. G.; Whitesides, G. M. *J. Phys. Chem.* **1995**, *99*, 7663-7676.
- (26) Dubois, L. H.; Zegarski, B. R.; Nuzzo, R. G. *J. Am. Chem. Soc.* **1990**, *112*, 570-579.
- (27) Snyder, R. G.; Strauss, H. L.; Elliger, C. A. *J. Phys. Chem.* **1982**, *86*, 5145-5150.
- (28) Koenig, J. L.; Angood, A. C. *J. Polym. Sci., Part A-2* **1970**, *8*, 1787-1796.
- (29) Both *molten* and *amorphous* are used to characterize the state of poly(ethylene glycol) at temperatures exceeding 350 K, because the spectra are considerably different from that of the crystalline polymer at lower temperatures (refs 2, 28). The helical splitting in the Raman spectra observed in the crystalline state disappears, and frequency shifts are observed. These changes indicate a loss of order and an appearance of added rotational isomers of trans, trans, trans conformations.
- (30) Matsuura, H.; Fukuhara, K. *J. Polym. Sci., Part B* **1986**, *24*, 1383-1400.
- (31) Bellamy, L. J. *The Infrared Spectra of Complex Molecules*; Chapman & Hall: London, 1980.

(32) Minimum immersion times for the formation of complete, protein resistant EG6-OH monolayers varied from 15 s to 10 min. Similar differences by several orders of magnitude in adsorption kinetics have been observed for unfunctionalized alkanethiolates. See for example: Pan, W.; Durning, C. J.; Turro, N. J. *Langmuir* **1996**, *12*, 4469–4473, and references cited therein.

(33) Nuzzo, R. G.; Dubois, L. H.; Allara, D. L. *J. Am. Chem. Soc.* **1990**, *112*, 558–564.

(34) Nuzzo, R. G.; Fusco, F. A.; Allara, D. L. *J. Am. Chem. Soc.* **1987**, *109*, 2358–2367.

(35) The deconvolution routine was started with the CH-stretching mode peak frequencies of the eight most dominant bands of polycrystalline alkanethiols as an initial guess. The line shape of the peaks was fixed as 50% Gaussian and 50% Lorentzian, and their half-widths and exact frequencies in the alkanethiolate spectrum were determined with a least-squares fitting routine.

(36) Miyazawa, T.; Fukushima, K.; Ideguchi, Y. *J. Chem. Phys.* **1962**, *37*, 2764–2776.

(37) Spectra for amorphous PEG shows a broad band with a maximum at 1107  $\text{cm}^{-1}$  and a shoulder at 1140  $\text{cm}^{-1}$ . See for example: Dissanayake, M. A. K. L.; Frech, R. *Macromolecules* **1995**, *28*, 5312–5319.

(38) The COC-stretching mode of crystalline PEG is split into a sharp, parallel polarized band at 1107  $\text{cm}^{-1}$  and two perpendicular polarized bands at 1119 and 1149  $\text{cm}^{-1}$  (ref 36).

(39) Laibinis, P. E.; Whitesides, G. M. *J. Am. Chem. Soc.* **1992**, *114*, 1990–1995.

(40) C<sub>6</sub> and C<sub>10</sub> samples on Ag were sometimes discolored and XPS spectra revealed the formation of silver sulfides. The alkanethiolate reference curve for Ag 3d<sub>5/2</sub> shows only C<sub>12</sub>–C<sub>22</sub>, because the reproducibility of formation of monolayers was much better for the longer chain lengths (ref 15).

(41) Attenuation length means the thickness of material required to reduce the flux of the emitted photoelectrons by 1/e and is denoted by  $\lambda$ .  $\lambda$  is not identical with the inelastic mean free path except in the absence of elastic scattering.

(42) According to the empirical approximation that the energy dependence of the mean free path scales with the kinetic energy and that the energy exponent is in the range 0.7–0.8 for organic materials (Tanuma, S.; Powell, C. J. Penn, D. R. *Surf. Interface Anal.* **1993**, *20*, 77–89), the IMFP (determined with a Mg K $\alpha$  source) for the Ag 3d photoelectrons should be  $\sim 0.5$  Å lower than for the Au 4d photoelectrons.

(43) Tanuma, S.; Powell, C. J.; Penn, D. R. *Surf. Interface Anal.* **1993**, *21*, 165–176.

(44) Hansen, H. S.; Tougaard, S.; Biebuyck, H. J. *Electron Spectrosc. Relat. Phenom.* **1990**, *58*, 141–158.

(45) Tanuma, S.; Powell, C. J.; Penn, D. R. *Surf. Interface Anal.* **1993**, *21*, 165–176.

(46) Laibinis, P. E.; Bain, C. D.; Whitesides, G. M. *J. Phys. Chem.* **1991**, *95*, 7017–7021.

(47) Jablonski, A.; Tilinin, I. S.; Powell, C. J. *Phys. Rev. B* **1996**, *54*, 10927–10937.

(48) Tanuma et al. analyzed the IMFP for various organic compounds and found that the IMFP can be predicted from the number of valence electrons per molecular unit, molecular weight, density, and bandgap energy for nonconductors. The number of valence electrons is the same for a propylene unit or an ethylene glycol unit. The other parameters (density, atomic weight) are similar or have only little influence on the IMFP. We therefore expect that the IMFP for the oligo(ethylene glycol)s should be the same within experimental error than for unfunctionalized alkanethiolates. Tanuma, S.; Powell, C. J.; Penn, D. R. *Surf. Interface Anal.* **1993**, *21*, 165–176.

(49) The effective molecular length scale in Figure 6 does not include the sulfur atom; we assumed the attenuation by the sulfur atoms as equivalent to that for 1.5 methylene units and corrected the relative thicknesses accordingly. For the surface coverage in molecules per  $\text{nm}^2$ , the relative difference between model and experiment might be somewhat smaller, because the theoretical values assume a homogeneous film density and do not include defects and domain boundaries.

(50) Fenter, P.; Eisenberger, P.; Li, J.; Camillone, N., III; Bernasek, S.; Scoles, G.; Ramanarayanan, T. A.; Liang, K. S. *Langmuir* **1991**, *7*, 2013–2016.

(51)  $n = 13$  for EG6-OH;  $n = 8$  for EG3-OMe.

(52) Horbett, T. A. *Adsorption to Biomaterials from Protein Mixtures*. In *Proteins at Interfaces: Physicochemical and Biochemical Studies*; Brash, J. L., Horbett, T. A., Eds.; ACS Symposium Series 343; American Chemical Society: Washington, DC, 1987; pp 239–260, and references cited therein.

(53) Corno, C.; Ghelli, S.; Perego, G.; Platone, E. *Colloid Polym. Sci.* **1991**, *269*, 1133–1139.

(54) Dubois, L. H.; Zegarski, B. R.; Nuzzo, R. G. *J. Chem. Phys.* **1993**, *98*, 678–688.

(55) Fenter, P.; Eisenberger, P.; Liang, K. S. *Phys. Rev. Lett.* **1993**, *70*, 2447–2450.

(56) Dhirani, A.; Hines, M. A.; Fisher, A. J.; Ismail, O.; Guyot-Sionnest, P. *Langmuir* **1995**, *11*, 2609–2614.

(57) Ulman, A. *Chem. Rev.* **1996**, *96*, 1533–1554.

(58) Matsuura, H.; Fukuhara, K. *J. Mol. Struct.* **1985**, *126*, 251–260.

(59) Lopez, G. P.; Biebuyck, H. A.; Härter, R.; Kumar, A.; Whitesides, G. M. *J. Am. Chem. Soc.* **1993**, *115*, 10774–10781.

(60) Szeleifer, I. *Curr. Opin. Solid State Mater. Sci.* **1997**, *2*, 337–344.

(61) Szeleifer, I. *Biophys. J.* **1997**, *72*, 595–612.

(62) See ref 11.